scientific reports

Check for updates

OPEN

Pharmacological WEE1 inhibition as a strategy to overcome cisplatin resistance in non-seminoma testicular cancer: insights from preclinical models

Mariangela Tamburello[1,7], Caterina Boldini[1,7], Andrea Abate[1]✉, Valentina Salvi[2], Francesca Valcamonico[3], Marta Laganà[3], Deborah Cosentini[3], Nazareno R. Suardi[4], Giuseppe Mirabella[4], Barbara Altieri[5,6] & Sandra Sigala[1]

Testicular germ cell tumors are the most common solid malignancy in young adult males with non-seminomatous representing a clinically aggressive subtype. Although cisplatin (CP)-based chemotherapy is highly effective, a subset of patients develop resistance. This study explored a potential new treatment by targeting WEE1, a key cell-cycle regulator, using the drug adavosertib in non-seminoma cell models, aiming to overcome CP resistance. Two non-seminoma cell lines, NCCIT and NT2/D1, and their CP-resistant subclones (NCCIT-R and NT2/D1-R) were used. The effects of adavosertib and CP, alone or in combination, on cell viability, cell-cycle progression, apoptosis, and DNA damage markers was assessed. WEE1 was expressed in non-seminoma cell models. Adavosertib reduced cell viability in a dose-dependent manner across all cell models in both 2D and 3D cultures. IC_{50} values were in low micromolar range (NCCIT: 0.550 µM; NCCIT-R: 0.630 µM; NT2/D1: 0.415 µM; NT2/D1-R: 0.630 µM). Adavosertib altered cell-cycle distribution, increasing S-phase population. Western blot analysis revealed that inhibiting WEE1 increases CDK1 activity and mitotic marker pH3, indicating disrupted cell cycle control. This leads to replication stress and forces cells with DNA damage into early mitosis, causing mitotic catastrophe. The treatment also triggered higher levels of DNA damage and cell death, as shown by increased caspase activity and apoptosis markers (cleaved-PARP and cleaved-Caspase 3). In combination treatments, adavosertib enhanced CP efficacy across all models, including resistant lines. Overall, our results provide compelling preclinical evidence supporting the combination of WEE1 inhibition with standard chemotherapy as a promising strategy to overcome CP-resistance in non-seminoma testicular cancer.

Keywords Testicular cancer, Cisplatin resistance, WEE1 inhibitors, Adavosertib, Debio 0123, Combined treatment

Testicular cancer (TC) is a heterogeneous disease, with the majority (90–95%) arising from germ cells (GCTs), followed by sex cord-gonadal stromal tumours and secondary tumours[1]. Testicular germ cell tumours (TGCTs) account for 1–1.5% of all male cancers and are the most common malignancy in males aged 15–40 years[2], with incidence rates highest in Scandinavian and lowest in African and Asian populations[3]. According to the World Health Organization, TGCTs are classified into seminomas and non-seminomas, which differ markedly in treatment approaches and therapeutic response[4]. Seminomas are relatively homogeneous tumours derived

[1]Section of Pharmacology, Department of Molecular and Translational Medicine, University of Brescia, Brescia, Italy. [2]Department of Molecular and Translational Medicine, University of Brescia, Brescia, Italy. [3]Oncology Unit, Department of Medical and Surgical Specialties, Radiological Sciences, and Public Health, University of Brescia at ASST Spedali Civili di Brescia, Brescia, Italy. [4]Urology Unit, Department of Medical and Surgical Specialties, Radiological Sciences, and Public Health, University of Brescia at ASST Spedali Civili di Brescia, Brescia, Italy. [5]Division of Endocrinology and Diabetes, Department of Internal Medicine I, University Hospital, University of Würzburg, Würzburg, Germany. [6]Bavarian Cancer Research Center (BZKF), Würzburg, Germany. [7]Mariangela Tamburello and Caterina Boldini equally to this work and are co-primary authors. ✉email: andrea.abate@unibs.it

from embryonic germ cells, whereas non-seminomas are often heterogeneous, comprising various histological elements such as embryonal carcinoma, yolk sac tumour, choriocarcinoma, and teratoma[5].

Nowadays, the standard treatment of TGCTs involves orchiectomy followed, if needed, by cisplatin (CP)-based chemotherapy and/or radiotherapy, according to cancer histology and disease stage. Low-risk patients are often managed with active surveillance, while high-risk cases typically receive CP-based chemotherapy regimens such as BEP (bleomycin, etoposide, and cisplatin)[6]. TGCTs are highly sensitive to CP, with survival rates exceeding 95%[7], and even patients relapsing or presenting disseminated disease are effectively treated with this agent, given in several successive treatment courses, if needed[8], resulting in only 3–5% of patients failing to respond completely to CP-based treatment[7].

The two key features of TGCTs associated with their high sensitivity to CP are insufficient DNA repair of CP-induced damage and a hypersensitive apoptotic response[6]. In contrast, CP resistance in TGCTs is a multifactorial process, involving upregulation of DNA damage response (DDR) pathways[9], which is considered the main source of resistance to DNA-damaging treatments in oncology[10].

Despite excellent overall survival rates, the treatment of CP-refractory or relapsed TGCTs remains a major clinical challenge. Therefore, developing novel therapeutic strategies is essential to improve outcomes in these "difficult-to-treat" patients.

Recently, our group identified the cyclin-dependent kinase 5 (CDK5) as a contributor to chemotherapy resistance in CP-resistant models of TGCTs, as it takes part in the DDR process. We demonstrated that CDK5 is overexpressed in CP-resistant cell models compared to their wild-type counterparts, suggesting its role in mediating resistance. We also showed that the CDK inhibitor dinaciclib, when combined with CP, enhances the sensitivity of non-seminomatous TGCTs to treatment, highlighting CDK5 as a potential therapeutic target. Moreover, several preclinical studies have demonstrated that inhibition of cell cycle regulators can induce replication stress, DNA damage accumulation, and ultimately cell death in TGCTs cell lines[11–13].

In the broader context of DDR regulators, WEE1 has emerged as another attractive target. WEE1 is a tyrosine kinase that regulates both the G2/M and S-phase checkpoints, by inhibiting CDK1 through phosphorylation at Tyr15. This regulation ensures proper DNA replication during S-phase and controlled progression through G2, helping to reduce replication stress and allowing time for DNA repair before mitosis[14,15]. From this perspective, WEE1 inhibition may potentiate DNA-damaging therapies such as chemotherapy and radiotherapy, by forcing cells to enter mitosis with unrepaired DNA, ultimately triggering mitotic catastrophe and cell death[14].

Until recently, the only WEE1 inhibitor evaluated in clinical trials was adavosertib (AZD1775), which has been tested across multiple cancer types, including ovarian, breast, and gastrointestinal cancers[16]. These studies investigate its use both as monotherapy and in combination with standard treatments such as chemotherapy and radiation[17–21]. While initial results were promising, some trials reported increased rates of grade 3 toxicities, including sepsis, which led to the discontinuation of adavosertib in 2022 due to safety concerns[22].

More recently, a new WEE1 inhibitor, Debio 0123, has entered clinical development. Preliminary data suggest a manageable safety profile, maintaining strong interest in the WEE1 inhibition as a therapeutic strategy[23].

In this study, we used adavosertib as a pharmacological tool to evaluate the impact of WEE1 inhibition in CP-sensitive and -resistant non-seminomatous TGCTs cell models, both as monotherapy and in combination with CP. The effect on the cell viability was as well assessed with another WEE1 inhibitor, namely Debio 0123.

Results

WEE1 expression and effect of WEE1 inhibition in wild-type NCCIT and NT2/D1 cells and in CP-R subclones

Since adavosertib inhibits the WEE1 tyrosine kinase, the expression of this target and other related proteins was first evaluated in NCCIT and NT2/D1 CP-sensitive cells (wild-type cells) and in their respective CP-resistant subclones, defined as NCCIT-R and NT2/D1-R, which represent the experimental cell models of CP-sensitive/CP-resistant non-seminoma used in this study.

Our results in Fig. 1A and B shown that WEE1 expression in NCCIT-R cells was 3.04-fold higher than in wild-type cells ($p < 0.05$), while a 1.99-fold increase of protein levels was found in NT2/D1 compared to the resistant subclone ($p < 0.001$). Overall, these data demonstrate that WEE1 is expressed in non-seminoma models and lays the foundation for studying the effect of adavosertib. The basal expression of WEE1-pathway–related proteins is shown in Supplementary Fig. 1.

The CP-sensitive/resistant non-seminoma cell models were treated with increasing concentrations of adavosertib and Debio 0123, and the effect on cell viability was evaluated. In both CP-sensitive and CP-resistant NCCIT and NT2/D1 (Fig. 1C,D), adavosertib induced a concentration-dependent reduction in cell viability. In comparison with adavosertib, Debio 0123 proved less effective in reducing cell viability, requiring higher, but still similarly ranged, concentrations to reach comparable maximal effects (Supplementary Fig. 2). A sigmoidal dose-response function was applied to calculate the IC_{50} values (Table 1 and Supplementary Table 1). In addition, we investigated the components of the WEE1 pathway and its inhibition by adavosertib and Debio 0123 in two other cell types: 833-K cells, which were established from a metastasis of a human TGCT, and TCAM-2 cells, which are derived from a TGCT. The results are reported in Supplementary Figs. 3–4 and Supplementary Table 2.

Adavosertib induced changes in the cell-cycle distribution in NCCIT and NT2/D1 wild-type and CP-R cells

WEE1 is a key regulator of the replication stress response, promoting cell cycle arrest at the intra-S and G2/M checkpoints by phosphorylating CDK1 and CDK2. This action ensures accurate DNA replication and repair before mitotic entry, thereby limiting replication stress. To evaluate whether adavosertib could affect the cell-cycle distribution, cells were treated with the adavosertib IC_{50} concentrations for 24 h and 48 h and analyzed by flow cytometry.

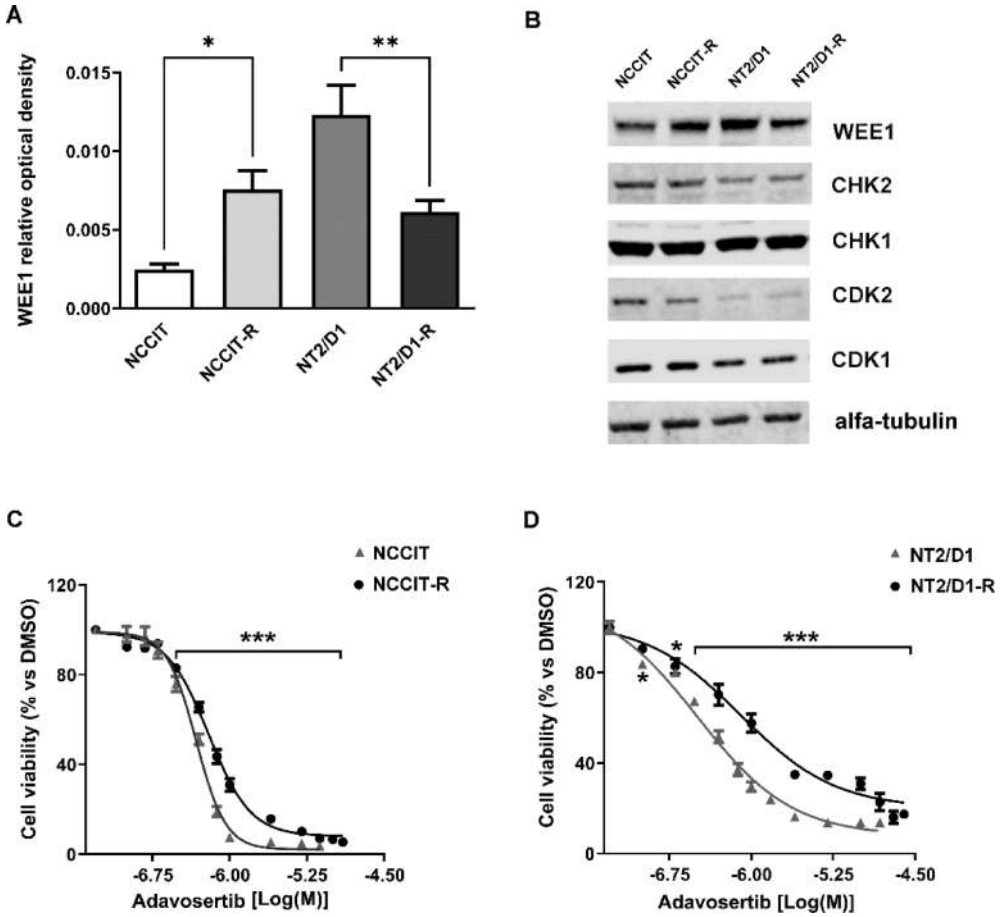

Fig. 1. Expression levels of WEE1 and WEE1-pathway–related proteins in non-seminoma cells (**A**) WEE1-levels quantification results are presented as a relative optical density means ± SD of three independent experiments, $^{**}p < 0.001$, $^{*}p < 0.05$ versus sensitive subclones. Original blots are presented in Supplementary Fig. 7 (**B**) Representative Western blot results of various WEE1-pathway–related proteins are shown. Original blots are presented in Supplementary Fig. 8 and quantification results are shown in Supplementary Fig. 1. Effect of adavosertib on (**C**) NCCIT/-R and (**D**) NT2/D1/-R cells. Cell viability assay was assessed after treatment with increasing concentrations of adavosertib for 48 h, as described in Methods. Results are expressed as the percentage of viable cells vs. untreated cells (DMSO control). Data are the mean ± SEM of three experiments performed in triplicate. $^{***}p < 0.0001$; $^{*}p < 0.05$ compared to untreated cells.

Cell line	Adavosertib
NCCIT	0.55 µM (95% CI 0.44–0.68 µM)
NCCIT-R	0.63 µM (95% CI 0.59–0.67 µM)
NT2/D1	0.42 µM (95% CI 0.35–0.49 µM)
NT2/D1-R	0.63 µM (95% CI 0.46–0.86 µM)

Table 1. IC_{50} values of adavosertib in non-seminoma cell lines.

As shown in Fig. 2A, adavosertib treatment reduced the proportion of cells in the G1 phase while promoting S-phase accumulation, suggesting cell cycle arrest in S phase. In both NCCIT and NCCIT-R models, a decreasing trend in G1-phase cells was observed at 24 and 48 h, with a corresponding increase in the S-phase population. NT2/D1 cells showed a modest reduction in G1-phase cells at 24 h and a slight increase at 48 h, along with consistent S-phase accumulation at both time points. In NT2/D1-R cells, adavosertib treatment led to a two-fold increase in the S-phase fraction at 24 h ($p < 0.05$), followed by a reduction at 48 h, which was accompanied by a three-fold increase in G2-phase cells ($p < 0.001$).

Consistent with these findings, western blot analysis showed reduced phosphorylation of CDK1 at Tyr15 at both 24 and 48 h post-treatment, indicating increased CDK1 activity associated with increased histone H3 phosphorylation at Ser10, a marker of mitosis. In parallel, adavosertib treatment enhanced phosphorylation of

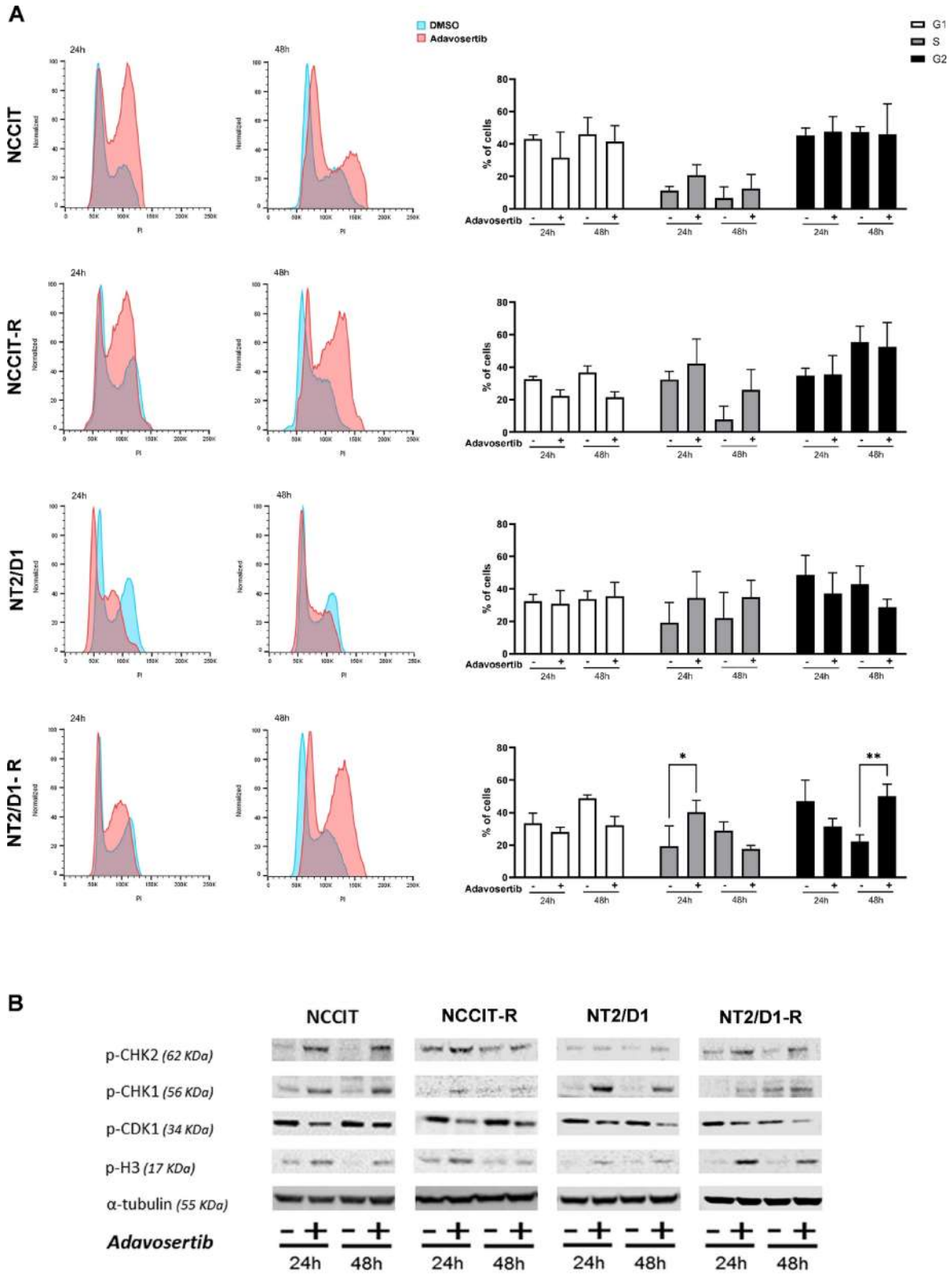

checkpoint kinases CHK1 and CHK2, suggesting activation of alternative checkpoint pathways as a potential compensatory mechanism (Fig. 2B and Supplementary Fig. 5).

These results indicate that WEE1 inhibition disrupted the cell cycle checkpoints, caused errors during S-phase, and forced cells with unrepaired DNA damage into premature mitosis, often leading to a mitotic catastrophe.

◀**Fig. 2**. (**A**) Cell cycle analysis of NCCIT, NCCIT-R, NT2/D1, and NT2/D1-R cells after 24 and 48 h of exposure to the IC_{50} concentration of adavosertib. Left panels show cell cycle distribution peaks for DMSO- and adavosertib-treated cells; right panels display corresponding histograms indicating the percentage of cells in each phase of the cell cycle. Data represent the mean ± SD of three independent experiments performed in triplicate. $^{*}p < 0.05$; $^{**}p < 0.001$ versus untreated controls. (**B**) Representative western blots of cell cycle regulators after 24 and 48 h of adavosertib treatment in non-seminoma cell lines. All Western blot analyses were conducted in parallel using the same samples. For each gel, the samples corresponding to the biological triplicates were loaded. The results from all triplicates were used to generate the quantification graphs provided in Supplementary Fig. 5. The most representative blots were selected, cropped, and included in the figure. Original blots are presented in Supplementary Figs. 9, 10 and 11.

Adavosertib treatment induced apoptotic cell death in NCCIT and NT2/D1 wild-type and CP-R cells

The effect of adavosertib on apoptosis was also evaluated by quantifying the activity of caspase-3 and -7 using the Caspase-Glo 3/7 assay, which are key executioner enzymes in the final stages of apoptosis and widely recognized markers of programmed cell death.

Figure 3 illustrates the levels of activated caspase-3/7 following treatment with increasing concentrations of adavosertib for 24 and 48 h. Overall, caspase activity increased in a dose-dependent manner, with a more pronounced effect observed at 24 h compared to 48 h. Specifically, in NCCIT cells (A), treatment with 1 µM adavosertib for 24 h led to a significant 6.9-fold elevation in caspase activity relative to control, whereas the increase was reduced to threefold at 48 h, though still statistically significant. Similarly, in NCCIT-R cells (B), treatment with the highest dose of 10 µM adavosertib resulted in a 2.5-fold increase in caspase activity at 24 h, followed by a modest 1.2-fold increase at 48 h. In NT2/D1 (C) and NT2/D1-R cells (D), caspase activity increased by approximately 3.4- and 2.5-fold, respectively, after 24 h of treatment with the maximum concentration. However, after 48 h of treatment, no significant differences in caspase activity were observed compared to untreated controls, except at lower drug concentrations where slight increases were detected.

The activation of apoptosis following adavosertib treatment was confirmed via Western blot analysis, assessing the levels of cleaved PARP and cleaved caspase-3, both established markers of apoptotic processes. Adavosertib treatment led to a significant increase in cleaved PARP levels across all tested models, with the most pronounced effects observed at 24 h. At 48 h, elevated cleaved PARP levels persisted, reaching statistical significance notably in NCCIT cells (Supplementary Fig. 6). Similarly, cleaved caspase-3 levels were elevated in all cell models at both 24 and 48 h post-treatment with adavosertib at their respective IC_{50} concentrations, indicating sustained apoptotic activation (Fig. 3E and Supplementary Fig. 6).

Additionally, we evaluated the phosphorylation of histone H2AX (Ser139), a marker of DNA double-strand breaks, to assess DNA damage accumulation resulting from WEE1 inhibition. Adavosertib treatment increased p-H2AX levels in all cell lines at both 24 and 48 h, with statistical significance for both wild-type subclones (Supplementary Fig. 6). Collectively, these results suggest that WEE1 inhibition compromised DNA damage repair mechanisms, leading to mitotic catastrophe and subsequent apoptotic cell death (Fig. 3E and Supplementary Fig. 6).

Effect of combined treatment of adavosertib and CP in NT2/D1 and NCCIT-sensitive and CP-resistant cells

To explore whether adavosertib could potentiate the cytotoxic effect of CP, the cornerstone of standard treatment for TC, we conducted combination treatment experiments in both CP-sensitive and CP-resistant non-seminoma cell lines. Cells were treated with increasing concentrations of CP alone or in combination with adavosertib at either ½ IC_{50} or IC_{50} concentrations. Cell viability was measured 48 h post-treatment to assess the cytotoxic effects of the single and combined treatments. The resulting concentration–response curves are presented in Fig. 4A and B (NCCIT-sensitive/R) and Fig. 4C and D (NT2/D1-sensitive/R).

To compare treatment responses across conditions and cell lines, we used two principal pharmacological parameters: efficacy and potency. These measures offer complementary perspectives, with efficacy capturing the maximal observed inhibition and IC_{50} reflecting drug potency. Moreover, we included the p53 mutation status of our models that can influence the response to treatment. Indeed, different from NT2/D1 cells, the NCCIT cells harbour a specific missense mutation within the DNA binding domain, leading to a change in the protein's structure and loss of its normal function. This mutation causes the p53 protein to become constitutively active, leading to a prolonged cell cycle arrest, and an increased resistance to apoptosis, while promoting proliferation and tumour growth[24,25].

As summarized in Table 2, combined treatment with CP and adavosertib, at both ½ IC_{50} and IC_{50} concentrations of adavosertib resulted in significantly increased efficacy in all cell lines except NT2/D1, where the combination did not enhance the cytotoxic effect beyond that of CP alone. Notably, the effect was particularly pronounced in the resistant subclones, which are, as expected, less responsive to CP as a single agent. This observation suggests a synergistic interaction or at least a sensitizing effect of adavosertib in the context of CP resistance (Table 2).

To further quantify this effect, we examined the shifts in IC_{50} values for CP when used in combination with adavosertib compared to CP alone. The data revealed a consistent and substantial reduction in CP IC_{50} in NCCIT, NCCIT-R and NT2/D1, with the most striking decrease was observed in NCCIT-R cells, where the CP IC_{50} dropped from 11.65 to 1.99 µM when combined with adavosertib at its IC_{50} concentration, indicating an approximately six-fold increase in CP sensitivity (Table 2). In the NT2/D1-R model, however, it was not possible to determine an accurate IC_{50} value under combination conditions. This is likely due to the steep

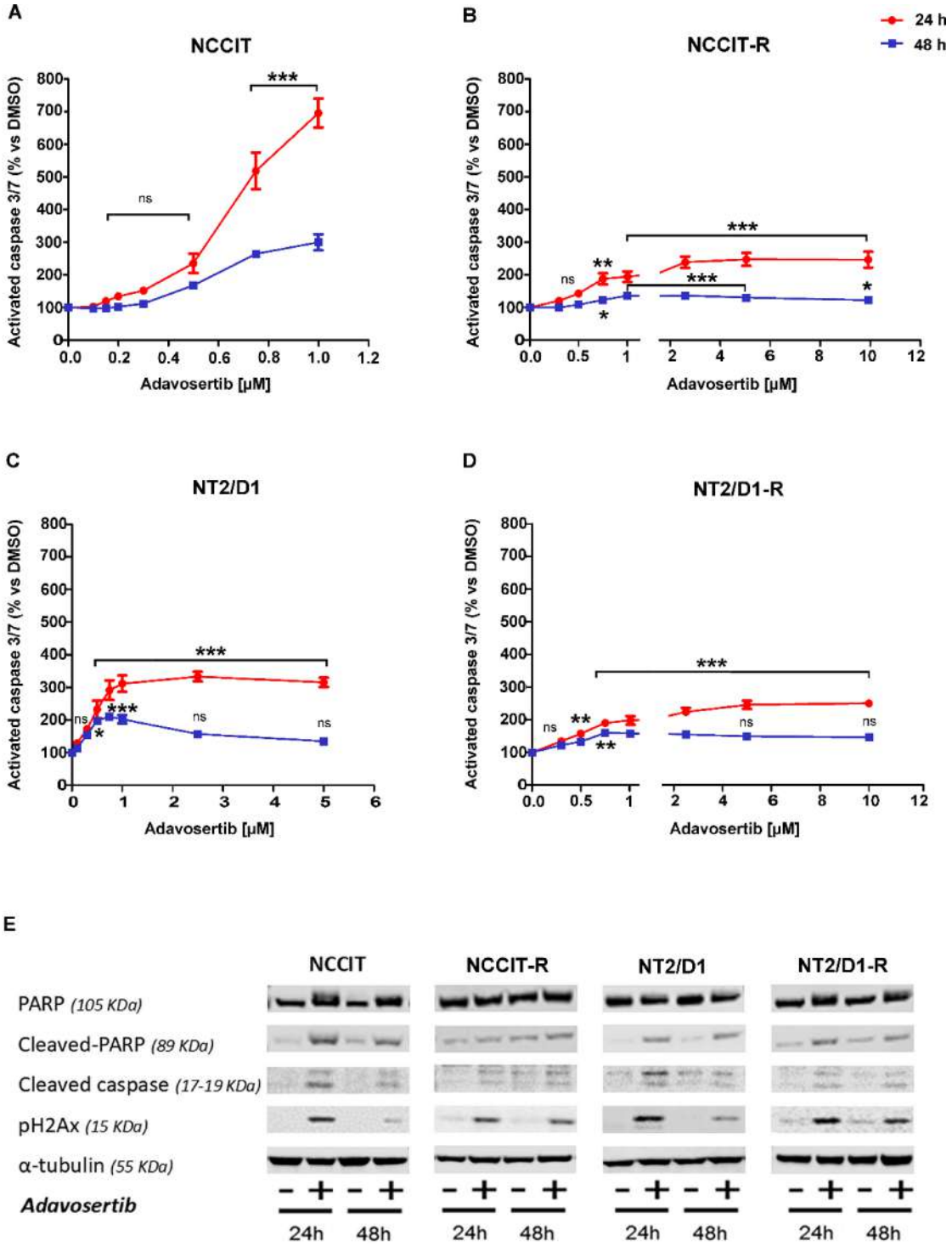

Fig. 3. Study of dose-dependent and time-dependent apoptotic induction of adavosertib in (**A**) NCCIT, (**B**) NCCIT-R, (**C**) NT2/D1, (**D**) NT2/D1-R cells. Data are the mean ± SEM of three experiments performed in triplicate. $^{*}p < 0.05$; $^{**}p < 0.001$; $^{***}p < 0.0001$ compared to untreated cells. (**E**) Representative western blots of apoptotic and DNA-damage markers after 24 and 48 h of exposure to IC_{50} of adavosertib in non-seminoma cell lines. Western blot quantifications are shown in Supplementary Fig. 6. Original blots are presented in Supplementary Figs. 11, 12 and 13.

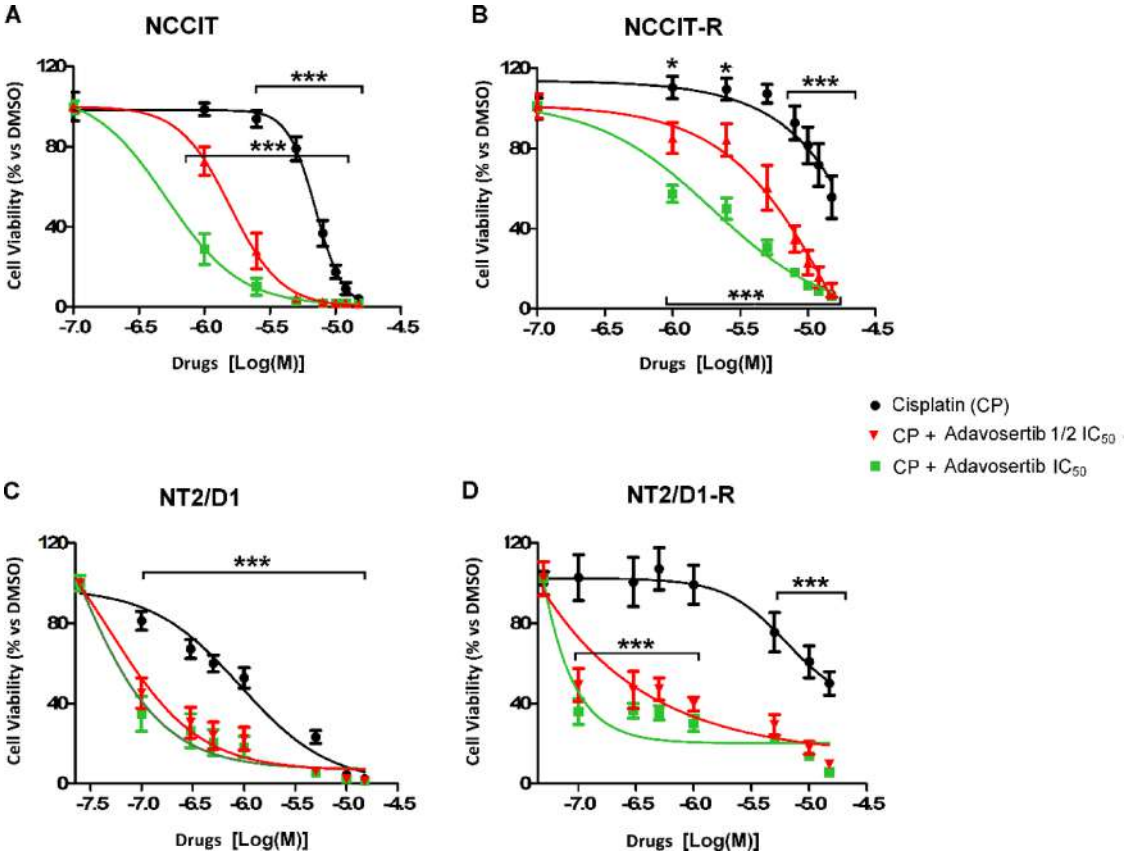

Fig. 4. Effect of combined treatment with CP and adavosertib on cell viability in NCCIT (**A**), NCCIT-R (**B**), NT2/D1 (**C**), NT2/D1-R (**D**). Results are expressed as the percentage of viable cells versus untreated cells (Ctrl) ± SEM. $^{*}p < 0.05$; $^{***}p < 0.0001$ versus untreated cells.

Cell line and p53 mutation status	Treatment	Efficacy (% ± SD)	IC_{50} (μM, 95% CI)
NCCIT mtp53: R248Q	CP	95.8% ±1.3	7.04 μM (95% CI 6.8–7.3 μM)
	CP + adavosertib ½ IC_{50}	98.3% ± 0.6***	1.58 μM (95% CI 1.4–1.7 μM)
	CP + adavosertib IC_{50}	97.9% ± 1.3**	0.51 μM (95% CI 0.4–0.7 μM)
NCCIT-R mtp53: R248Q	CP	45.6% ± 10.1	11.65 μM (95% CI 8.8–15.5 μM)
	CP + adavosertib ½ IC_{50}	93.6% ± 2.4***	7.75 μM (95% CI 6.28–9.6 μM)
	CP + adavosertib IC_{50}	90.7% ± 3.4***	1.99 μM (95% CI 1.4–2.9 μM)
NT2/D1 wtp53	CP	97.7% ± 1.1	0.914 μM (95% CI 0.8–1.1 μM)
	CP + adavosertib ½ IC_{50}	98.6% ± 0.1	0.049 μM (95% CI 0.03–0.08 μM)
	CP + adavosertib IC_{50}	98.6% ± 0.1	0.019 μM (95% CI 0.01–0.04 μM)
NT2/D1-R wtp53	CP	50% ± 5.8	6.42 μM (95% CI 3.8–11 μM)
	CP + adavosertib ½ IC_{50}	90.4% ± 1.81***	–
	CP + adavosertib IC_{50}	93.6% ± 0.6***	–

Table 2. Efficacy and IC_{50} of cisplatin (CP) alone and in with adavosertib in non-seminoma cell lines. Efficacy values are reported as mean ± SD. $^{**}p < 0.001$, $^{***}p < 0.0001$ versus efficacy of CP.

response curve and high level of cell death observed even at the lowest CP concentrations tested, particularly when adavosertib was co-administered (Fig. 4D). Despite this limitation, the efficacy data showed a clear and statistically significant increase in cytotoxicity with the combination treatment, consistent with the trends observed in the other cell lines[26,27] and supporting the conclusion that adavosertib enhanced CP activity even in resistant models. Consistent with these findings, comparable effects were also observed in 833-K and TCAM-2 cells treated with the CP–adavosertib combination, as shown in Supplementary Fig. 4 and Supplementary Table 3, further confirming the robustness of this response across different TGCT models.

Taken together, these results support the rationale for combining WEE1 inhibition with cisplatin in non-seminoma TC, particularly as a strategy to overcome chemoresistance.

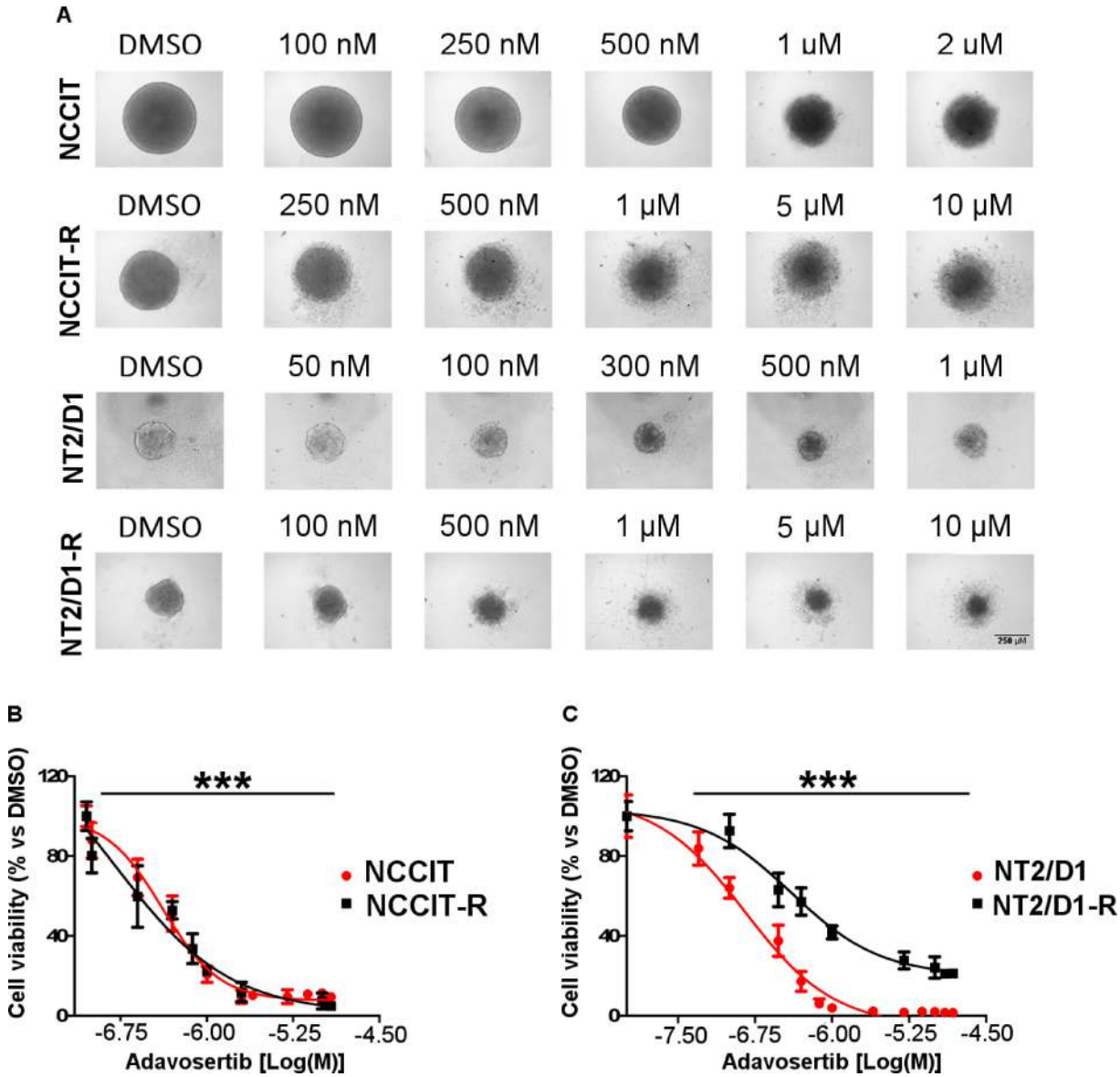

Fig. 5. (**A**) Representative images of spheroids treated with increasing concentrations of adavosertib. The images were acquired using an optical microscope equipped with a 10× objective lens. Effect of adavosertib on 3D models of (**B**) NCCIT/-R and (**C**) NT2/D1/-R in terms of cell viability. Data are the mean ± SEM of three experiments performed in triplicate. ***$p < 0.0001$ compared to untreated spheroids.

Effect of Adavosertib treatment on NT2/D1/-R and NCCIT/-R cell spheroids

In addition to conventional 2D cell culture models, the effect of adavosertib on cell viability was further investigated using a 3D culture system, specifically, multicellular tumour spheroids.

In this study, spheroids were generated from non-seminoma TGCTs cell lines and treated with increasing concentrations of adavosertib. Cell viability was assessed after 72 h using the CellTiter-Glo® 3D Cell Viability Assay, which is specifically optimized for spheroid systems. The results of the viability assay are presented in Fig. 5B and C.

Consistent with the findings in 2D adherent cultures, adavosertib demonstrated a concentration-dependent cytotoxic effect in the 3D spheroid model. These findings strengthen the drug's antitumour activity and suggest that WEE1 inhibition retained its effectiveness in more complex, physiologically relevant conditions that more closely resemble the in vivo tumour setting.

Moreover, qualitative analysis of spheroid morphology via light microscopy provided further insight into the effects of adavosertib on 3D tumour architecture. As shown in Fig. 5A, untreated spheroids retained their characteristic compact and spherical shape with well-defined borders. In contrast, spheroids treated with increasing concentrations of adavosertib exhibited a progressive loss of structural integrity. Specifically, we observed a marked disruption of spheroid margins, reduction in compactness, and an irregular contour, indicative of compromised cellular cohesion. In parallel, widespread necrotic areas became increasingly evident,

likely resulting from drug-induced cell lysis and subsequent release of intracellular contents into the extracellular space. These morphological alterations are consistent with the biochemical evidence of decreased viability and further support the cytotoxic activity of adavosertib.

Overall, the 3D spheroid model confirmed and extended the cytotoxic profile of adavosertib observed in 2D monolayer cultures. The alignment of results across both systems strengthens the reliability of the data and underscores the potential of adavosertib as an effective therapeutic agent in non-seminoma TC, including in more clinically relevant tumour architectures.

Discussion

In this study, we investigated the role of WEE1 and the therapeutic potential of its inhibition by adavosertib in CP-sensitive and CP-resistant non-seminoma cell models. We first examined WEE1 protein expression in NCCIT and NT2/D1 cell lines and their respective CP-resistant counterparts (NCCIT-R and NT2/D1-R). Our data demonstrate that WEE1 is expressed in all models. Consistently, data from the Human Protein Atlas indicate moderate to high WEE1 expression in most TGCTs. (https://www.proteinatlas.org/ENSG00000166483-WEE1/cancer).

Focusing on differences between CP-sensitive and -resistant subclones, WEE1 was significantly overexpressed in the resistant NCCIT-R cells compared to their wild-type counterparts. Our findings align with previous reports describing chemotherapy-induced upregulation of WEE1 as a potential adaptive mechanism that enhances DNA damage repair and promotes survival[28]. Conversely, in the NT2/D1 model, WEE1 was more highly expressed in wild-type cells than in the resistant subclone.

Overall, our findings confirm that WEE1 is expressed across cell models, with expression patterns possibly reflecting differences in resistance mechanisms and cellular context.

Functionally, adavosertib demonstrated strong anticancer activity across all tested cell lines, showing concentration-dependent cytotoxicity in both 2D and 3D culture systems. The low nanomolar IC_{50} values, below clinically achievable plasma concentrations[17,29], highlight its potent and uniform efficacy, even in complex 3D tumour models[30], supporting its potential for further clinical investigation.

Mechanistically, WEE1 inhibition disrupted cell cycle progression, primarily by reducing the G1-phase population and promoting S-phase accumulation, indicative of S-phase arrest. In NCCIT and NCCIT-R cells, this effect was consistent over time, while NT2/D1 and NT2/D1-R cells showed distinct temporal dynamics, with NT2/D1-R cells also displaying a significant increase in the G2-phase fraction at later time points. These results are in line with WEE1's established role in regulating intra-S and G2/M checkpoints via phosphorylation of CDK1 and CDK2 and support the hypothesis that WEE1 inhibition forces cells with unresolved DNA damage into premature mitosis[31]. This was further supported by western blot analyses: reduced phosphorylation of CDK1 (Tyr15) and increased levels of phosphorylated histone H3 (Ser10) confirmed mitotic entry[32], while elevated phosphorylation of CHK1 and CHK2 pointed to activation of compensatory DNA damage checkpoints[33].

Importantly, WEE1 inhibition led to pronounced apoptotic activation, as demonstrated by increased caspase-3/7 activity, cleavage of PARP and caspase-3, and accumulation of pH2AX, a marker of DNA double-strand breaks[34]. The early peak in apoptotic markers at 24 h, particularly in NCCIT cells, followed by reduced activation at 48 h, may reflect either the rapid onset of mitotic catastrophe or the selection of surviving subpopulations. This trend was also confirmed by other studies, which highlighted a temporal peak in caspase activity around 24 h, followed by a subsequent decrease, thereby identifying 24 h as the optimal time point for measurement[35,36].

Successively, we evaluated the effect of combining adavosertib with cisplatin, the current standard of care for testicular cancer[37]. Combination treatment experiments revealed that co-administration of adavosertib with cisplatin significantly enhanced therapeutic efficacy in nearly all tested models. The effect was particularly striking in CP-resistant cells (NCCIT-R and NT2/D1-R as well as 833-K and TCAM-2 cells), where single-agent cisplatin showed limited cytotoxicity. In NCCIT-R and TCAM-2 cells, for instance, combining cisplatin with adavosertib at its IC_{50} concentration reduced the cisplatin IC_{50} by approximately sixfold, from 11.65 to 2 µM, indicating a substantial restoration of CP sensitivity. Similarly, in NT2/D1-R and 833-K cells, combination treatment markedly increased cytotoxicity, although precise IC_{50} values could not be calculated due to the steep dose–response and high efficacy observed at even low doses.

The NT2/D1 wild-type cells did not exhibit further cytotoxicity with the combination compared to CP alone, suggesting that the benefit of WEE1 inhibition may be more pronounced in the setting of acquired resistance in cancer. The different impact of the combination treatment between NCCIT and NT2/D1 could be explained by the presence of mutated p53 in the NCCIT cell model and wild type p53 in NT2 cells[38]. Several preclinical studies have shown that adavosertib exhibits synergistic activity with chemotherapy, particularly in p53-deficient cancer cells[39–43], where cells are completely dependent on the WEE1 for G2/M checkpoint control[44]. However, different from other cancer types, p53 mutations are rarely observed in TGCTs[45].

Our findings are of significant interest as they highlight the potential of combining WEE1 inhibition with CP. This aligns with a broader trend observed in over 30 clinical trials listed on ClinicalTrials.gov investigating adavosertib across various cancer types, most of which evaluate its use in combination with DNA-damaging agents such as carboplatin, cisplatin, docetaxel, 5-fluorouracil, gemcitabine, irinotecan, paclitaxel, pemetrexed, temozolomide, topotecan, or radiotherapy[20,29,44,46–48].

These findings suggest a potential synergistic or sensitizing effect of adavosertib when combined with DNA-damaging agents, supporting its use as an adjunct to enhance chemotherapy efficacy in refractory TC. This strategy may improve responsiveness in treatment-resistant tumours. However, optimizing the safety profile and the selectivity of WEE1 inhibitors remains a challenge. It is important to say that adavosertib development was discontinued in 2022 due to dose-limiting toxicities[22]. However, concerns have emerged with also newer agents, like azenosertib, largely due to limited kinase selectivity and off-target PLK1/2 inhibition. Importantly,

next-generation WEE1 inhibitors such as Debio 0123 have been recently developed with improved selectivity, showing preliminary evidence of a better safety profile and potential efficacy in Phase 1 trials in patients with advanced solid tumors[23], reaffirming the therapeutic promise of WEE1 inhibition when paired with enhanced drug specificity. Consistent with these clinical observations, our results show that although Debio 0123 is less potent than adavosertib in reducing cell viability in some cell models, it achieves comparable maximal effects at concentrations that remain within the same order of magnitude. Furthermore, two other Phase 1 clinical studies are active to test Debio 0123 combined with the platinum-derivative carboplatin in advanced solid tumours (NCT03968653) or in recurrent/progressed after platinum-based therapy in small cell lung cancers (NCT05815160), to test the safety in the dose-escalation and a preliminary efficacy in the dose-expansion arm (www.clinicaltrials.gov, accessed May 13, 2025).

Conclusions

Overall, our data suggest that WEE1 is a druggable target in TGCT cancers, including CP-resistant setting. WEE1 inhibition with adavosertib compromises cell cycle control, disrupts DNA damage repair, and induces apoptotic cell death across all tested models. The enhancement of CP cytotoxicity by adavosertib in CP-resistant cell models further highlights the clinical potential of this combination to overcome chemoresistance in TGCT. As new WEE1 inhibitor compounds with better safety profile and target selectivity are now in clinical development, alone or combined with platinum-derivatives, our results would give a preclinical in vitro basis to suggest further investigations in the setting of TGCT.

Materials and methods

2D cell cultures

Cell lines

The NT2/D1 cell line (ATCC CRL-1973) was purchased from the *American Type Culture Collection* (ATCC, Manassas, VA) and cultured as indicated by the manufacturer. The NCCIT cell line and the CP-resistant subclones, NT2/D1-R and NCCIT-R, were kindly given by Pr. Bremmer (Gottingen, Germany) and cultured as suggested[49]. The 833-K cell line was kindly provided by B. Köberle (Karlsruhe Institute of Technology, Karlsruhe, Germany) and J. Masters (University College London, London, UK) while TCAM-2 from University of Naples. Culture medium and supplements were purchased from Merck (Darmstadt, Germany). All cell lines were periodically tested for mycoplasma and authenticated (BMR Genomics, Padova, Italia). Furthermore, CP-resistant subclones were treated with subtoxic doses of 1.25 µM CP for 3 days, followed by a 3-day washout period, to maintain drug resistance. Resistance to CP was periodically confirmed[49,50].

Single drug treatment

Cells (8000/well) were seeded in a 96-well plate. After 24 h, cells were treated for 48 h with increasing concentrations of adavosertib (NCCIT: 0.1–1 µM; NCCIT-R: 0.3–10 µM; NT2/D1: 0.1–5 µM; NT2/D1-R: 0.1–25 µM; 833-K: 0.5–30 µM; TCAM-2: 0.1–4 µM), or Debio-0123 (NCCIT: 3–20 µM; NCCIT-R: 2–15 µM; NT2/D1: 0.5–5 µM; NT2/D1-R: 1–15 µM; 833-K: 0.5–30 µM; TCAM-2:1–15 µM), according to the calculated doubling time[51]. Preliminary experiments were performed to evaluate the range of sensitivity to adavosertib across the different cell models. To test CP resistance, cells were treated with increasing concentrations of CP (0.05–36 µM). CP and adavosertib were purchased from Selleck Chemicals (Milan, Italy) and solubilized in dimethylformamide (DFM) and dimethyl sulfoxide (DMSO), respectively. At the end of the treatment period, cell viability was assessed using the CellTiter-Glo® Cell Viability Assay (Promega, Milan, Italy), following the manufacturer's protocol. An equal volume of CellTiter-Glo® Reagent was added to each well to achieve a final 1:1 ratio with the culture medium. To promote efficient cell lysis and reagent mixing, the plate was shaken for 2 min, followed by a 10-min incubation at room temperature to allow the luminescent signal to stabilize. Luminescence was then measured using the EnSight™ Multimode Plate Reader (PerkinElmer, Milan, Italy).

Cell-cycle analysis

To investigate the biological role of adavosertib, cell cycle state was analyzed in nonseminoma tumour cells. Cells (8×10^5) were seeded in 6-well plates, allowed to adhere for 24 h, and then treated with their respective IC_{50} value of adavosertib for 24 and 48 h. Cells were harvested using 0.05% Trypsin/EDTA, washed with ice-cold PBS and stained with the violet LIVE/DEAD Fixable Dead Cell Stain Kit (Thermo-Fisher Scientific, Milan, Italy). Untreated and treated cells were than fixed with ethanol (70%), treated with Rnase A (12.5 µg/mL) (Thermo-Fisher Scientific, Milan, Italy), stained with propidium iodide (40 µg/mL) (Invitrogen, Thermo-Fisher Scientific, Milan, Italy), and analyzed by flow cytometry using a MACSQuant16 Analyzer (Miltenyi Biotec GmbH, Bielefeld, Germany) for cell-cycle status. Data were analyzed using FlowJo v10.6.2 software (TreeStar, Ashland, OR, USA) with the Dean–Jett–Fox model (with sync-peak).

Caspase 3/7 assay

To assess the pro-apoptotic effect of adavosertib, cells were seeded at a density of 8000 cells per well in a 96-well plate and treated with increasing concentrations of adavosertib for 24 and 48 h. Apoptosis was evaluated by quantifying the activity of caspases 3 and 7 using the Caspase-Glo® 3/7 Assay (Promega, Milan, Italy), according to the manufacturer's instructions. At the end of the treatment period, an equal volume of Caspase-Glo® 3/7 Reagent was added to the culture medium in each well to achieve a final 1:1 ratio. To promote cell lysis and reagent mixing, the plate was gently shaken for 30 s, followed by a 1-h incubation at room temperature to allow the luminescent signal to stabilize. Luminescence was then measured using the EnSight™ Multimode Plate Reader (PerkinElmer).

Combined treatment with CP and adavosertib

To investigate the impact of the combined treatment with CP and adavosertib on non-seminoma cell viability, cells were seeded at 8000 cells per well in 96-well plates and exposed for 48 h to increasing concentrations of CP (NT2/D1 and NT2/D1-R: 0.1–15 μM; NCCIT and NCCIT-R:1–15 μM ; 833-K and TCAM-2: 5–35 μM). Treatments were performed in the presence or absence of adavosertib at concentrations corresponding to ½ IC_{50} and IC_{50} values previously determined for each cell line. At the end of the treatment period, cell viability was assessed using the CellTiter-Glo® Cell Viability Assay (Promega), as described above. To ensure a robust evaluation of treatment responses, two key pharmacological parameters were taken into account: efficacy, defined as the maximal inhibition of cell viability observed, and CP-IC_{50}, the CP concentration required to reduce cell viability by 50% of the maximum inhibitory effect observed in each cell line. These metrics provide complementary insights into drug response, with efficacy reflecting the maximal achievable effect and IC_{50} serving as a quantitative indicator of drug potency, allowing direct comparison of sensitivity across different treatment conditions and cell models.

3D cell cultures

Each cell line was cultured in a 96-well U-bottom plate specifically designed to prevent cell adhesion to the substrate, thereby promoting the spontaneous aggregation of cells into three-dimensional (3D) spheroids at the curved bottom of each well. This configuration facilitates the formation of uniform spheroids and better recapitulates the architecture of in vivo tumour. Prior to experimental treatments, preliminary optimization assays were conducted to determine the optimal seeding density and incubation time required for consistent and reproducible spheroid formation across all cell lines. Based on these results, a seeding density of 4000 cells per well was established as optimal. Cells were suspended in their respective culture media, as previously described, and seeded under sterile conditions. After 24 h, the cells had self-organized into compact spheroids, which were subsequently treated for 48 h with increasing concentrations of adavosertib. After preliminary experiments, the treatment ranges were as follows: NCCIT (0.1–2 μM), NCCIT-R (0.25–10 μM), NT2/D1 (0.05–1 μM), and NT2/D1-R (0.1–10 μM).

Spheroid viability was assessed using the CellTiter-Glo® 3D Cell Viability Assay (Promega), according to the manufacturer's instructions. At the end of the treatment period, an equal volume of CellTiter-Glo® 3D Reagent was added to each well to achieve a 1:1 ratio. Spheroids were then mechanically disaggregated using a multichannel pipette to facilitate cell lysis. Following a 25-min incubation at room temperature to allow stabilization of the luminescent signal, luminescence was measured using the EnSight™ Multimode Plate Reader (PerkinElmer). Prior to viability measurements, representative images of selected spheroids were acquired using an Olympus IX51 optical microscope (Olympus, Segrate, Italy) equipped with a 10× objective to visually assess spheroid morphology.

Western blot

Cells were homogenized in cold RIPA buffer, and total protein concentrations were determined by Bio-Rad Protein Assay (Bio-Rad Laboratories, Segrate, Italy). Equal amounts of proteins (30 μg) were separated by electrophoresis on a 4–12% NuPAGE bis-tris gel system (Life Technologies, Italy) and transferred onto a nitrocellulose membrane (GE Healthcare Italia, Milano, Italia). Membranes were reacted using the primary antibodies shown in Supplemental Table 4. Secondary anti-mouse (IRDye 680CW conjugated) and anti-rabbit (IRDye 800CW conjugated) antibodies (final concentration: 0.67 μg/mL; LI-COR Biosciences, Linloln, NE, USA) were applied for 1 h at room temperature. The specific signal was visualized using Odyssey Imaging System (LI-COR Biosciences, Lincoln, NE, USA) and the densitometry analysis was performed using the Image Studio TM Light V 5.2 Software (LI-COR Bio-sciences).

Statistical analysis

Statistical analysis was carried out using GraphPad Prism (version 10, GraphPad Software, La Jolla, CA, USA). Statistical analysis was carried out using one-way analysis of variance (ANOVA) and Bonferroni's multiple comparison test or Student's t-test. $p < 0.05$ was considered statistically significant. Unless otherwise specified, data are expressed as mean ± SD of at least three experiments run in triplicate.

Data availability

The datasets used and/or analysed during the current study available from the corresponding author on reasonable request.

Received: 13 June 2025; Accepted: 31 December 2025
Published online: 29 January 2026

References

1. Boccellino, M. et al. Testicular cancer from diagnosis to epigenetic factors. *Oncotarget* **8**(61), 104654–104663 (2017).
2. King, J., Adra, N. & Einhorn, L. H. Testicular cancer: Biology to bedside. *Cancer Res.* **81**(21), 5369–5376 (2021).
3. Rajpert-De Meyts, E. et al. Testicular germ cell tumours. *Lancet* **387**(10029), 1762–1774 (2016).
4. Oldenburg, J. et al. Testicular seminoma and non-seminoma: ESMO clinical practice guidelines for diagnosis, treatment and follow-up. *Ann. Oncol.* **24**(Suppl 6), 125–132 (2013).
5. Lobo, J. et al. Testicular germ cell tumors: Revisiting a series in light of the new WHO classification and AJCC staging systems, focusing on challenges for pathologists. *Hum. Pathol.* **82**, 113–124 (2018).
6. de Vries, G. et al. Testicular cancer: Determinants of cisplatin sensitivity and novel therapeutic opportunities. *Cancer Treat. Rev.* **88**, 102054 (2020).

7. Lobo, J., Jerónimo, C. & Henrique, R. Cisplatin resistance in testicular germ cell tumors: Current challenges from various perspectives. *Cancers (Basel)*. **12**(6), 1601 (2020).
8. O'Shaughnessy, M. J. et al. Late relapse of testicular germ cell tumors. *Urol. Clin. N. Am.* **42**(3), 359–368 (2015).
9. Goldstein, M. & Kastan, M. B. The DNA damage response: Implications for tumor responses to radiation and chemotherapy. *Annu. Rev. Med.* **66**, 129–143 (2015).
10. Esposito, F. et al. *Wee1 kinase: A potential target to overcome tumor resistance to therapy.* Int. J. Mol. Sci. 22(19), 10689. (2021).
11. Funke, K. et al. Transcriptional CDK inhibitors as potential treatment option for testicular germ cell tumors. *Cancers (Basel)*. **14**(7), 1690 (2022).
12. Rossini, E. et al. Cisplatin cytotoxicity in human testicular germ cell tumor cell lines is enhanced by the CDK4/6 inhibitor palbociclib. *Clin. Genitourin. Cancer*. **19**(4), 316–324 (2021).
13. Rossini, E. et al. The CDK inhibitor dinaciclib improves cisplatin response in nonseminomatous testicular cancer: A preclinical study. *Cells* **13**(5), 368 (2024).
14. Ghelli Luserna di Rorà, A. et al. A WEE1 family business: Regulation of mitosis, cancer progression, and therapeutic target. *J. Hematol. Oncol.* **13**(1), 126 (2020).
15. Rowley, R., Hudson, J. & Young, P. G. The wee1 protein kinase is required for radiation-induced mitotic delay. *Nature* **356**(6367), 353–355 (1992).
16. Krishnapriya, T. et al. WEE1 inhibition in cancer therapy: Mechanisms, synergies, preclinical insights, and clinical trials. *Crit. Rev. Oncol. Hematol.* **211**, 104710 (2025).
17. Do, K. et al. Phase I study of single-agent AZD1775 (MK-1775), a Wee1 kinase inhibitor, in patients with refractory solid tumors. *J. Clin. Oncol.* **33**(30), 3409–3415 (2015).
18. Méndez, E. et al. A phase I clinical trial of AZD1775 in combination with neoadjuvant weekly docetaxel and cisplatin before definitive therapy in head and neck squamous cell carcinoma. *Clin. Cancer Res.* **24** (12), 2740–2748 (2018).
19. Moore, K. N. et al. *Adavosertib with chemotherapy in patients with primary platinum-resistant ovarian, fallopian tube, or peritoneal cancer: An open-label, four-arm, phase II study.* Clin. *Cancer Res.* **28**(1), 36–44 (2022).
20. Cuneo, K. C. et al. Dose escalation trial of the Wee1 inhibitor adavosertib (AZD1775) in combination with gemcitabine and radiation for patients with locally advanced pancreatic cancer. *J. Clin. Oncol.* **37**(29), 2643–2650 (2019).
21. Liu, J. F. et al. *A Phase II Trial of the Wee1 Inhibitor Adavosertib (AZD1775) in Recurrent Uterine Serous Carcinoma* (American Society of Clinical Oncology, 2020).
22. Liu, J. et al. A phase IIb, open-label, single-arm, multicenter study assessing the efficacy and safety of adavosertib (AZD1775) as treatment for recurrent or persistent uterine serous carcinoma (039). *Gynecol. Oncol.* **176**, S33–S35 (2023).
23. Papadopoulos, K. P. et al. Results of a phase 1, dose-finding study of Debio 0123 as monotherapy in adult patients with advanced solid tumors: Safety, pharmacokinetic, and preliminary antitumor activity data. *J. Clin. Oncol.* **42**(16_suppl), 3120–3120 (2024).
24. Burger, H. et al. Expression of p53, p21/WAF/CIP, Bcl-2, Bax, Bcl-x, and bak in radiation-induced apoptosis in testicular germ cell tumor lines. *Int. J. Radiat. Oncol. Biol. Phys.* **41**(2), 415–424 (1998).
25. Timmerman, D. M. et al. The role of TP53 in cisplatin resistance in mediastinal and testicular germ cell tumors. *Int. J. Mol. Sci.* **22**(21), 11774 (2021).
26. Chen, D. et al. Wee1 inhibitor AZD1775 combined with cisplatin potentiates anticancer activity against gastric cancer by increasing DNA damage and cell apoptosis. *Biomed. Res. Int.* **2018**, 5813292 (2018).
27. De Witt Hamer, P. C. et al. WEE1 kinase targeting combined with DNA-damaging cancer therapy catalyzes mitotic catastrophe. *Clin. Cancer Res.* **17**(13), 4200–4207 (2011).
28. Slipicevic, A. et al. Wee1 is a novel independent prognostic marker of poor survival in post-chemotherapy ovarian carcinoma effusions. *Gynecol. Oncol.* **135**(1), 118–124 (2014).
29. Leijen, S. et al. Phase II study of WEE1 inhibitor AZD1775 plus carboplatin in patients with TP53-mutated ovarian cancer refractory or resistant to first-line therapy within 3 months. *J. Clin. Oncol.* **34**(36), 4354–4361 (2016).
30. Anu, V. et al. New frontiers in anti-cancer drug testing: the need for a relevant in vitro testing model. *NAM J.* **1**, 100003 (2025).
31. Matheson, C. J., Backos, D. S. & Reigan, P. Targeting WEE1 kinase in cancer. *Trends Pharmacol. Sci.* **37**(10), 872–881 (2016).
32. Elmaci, İ. et al. Phosphorylated histone H3 (PHH3) as a novel cell proliferation marker and prognosticator for meningeal tumors: A short review. *Appl. Immunohistochem. Mol. Morphol.* **26**(9), 627–631 (2018).
33. Stracker, T. H., Usui, T. & Petrini, J. H. Taking the time to make important decisions: The checkpoint effector kinases Chk1 and Chk2 and the DNA damage response. *DNA Repair. (Amst)*. **8**(9), 1047–1054 (2009).
34. van Attikum, H. & Gasser, S. M. Crosstalk between histone modifications during the DNA damage response. *Trends Cell. Biol.* **19**(5), 207–217 (2009).
35. Pan, Y. et al. Evaluation of pharmacodynamic biomarkers in a phase 1a trial of dulanermin (rhApo2L/TRAIL) in patients with advanced tumours. *Br. J. Cancer*. **105**(12), 1830–1838 (2011).
36. Wen, Y. et al. Chemotherapeutic-induced apoptosis: A phenotype for pharmacogenomics studies. *Pharmacogen Genom.*. **21**(8), 476–488 (2011).
37. Oldenburg, J. et al. Testicular seminoma and non-seminoma: ESMO-EURACAN clinical practice guideline for diagnosis, treatment and follow-up. *Ann. Oncol.* **33**(4), 362–375 (2022).
38. Burger, H. et al. Lack of correlation between cisplatin-induced apoptosis, p53 status and expression of Bcl-2 family proteins in testicular germ cell tumour cell lines. *Int. J. Cancer*. **73**(4), 592–599 (1997).
39. Bridges, K. A. et al. MK-1775, a novel Wee1 kinase inhibitor, radiosensitizes p53-defective human tumor cells. *Clin. Cancer Res.* **17**(17), 5638–5648 (2011).
40. Hirai, H. et al. Small-molecule Inhibition of Wee1 kinase by MK-1775 selectively sensitizes p53-deficient tumor cells to DNA-damaging agents. *Mol. Cancer Ther.* **8**(11), 2992–3000 (2009).
41. Hsu, W. H. et al. Checkpoint kinase 1 inhibition enhances cisplatin cytotoxicity and overcomes cisplatin resistance in SCLC by promoting mitotic cell death. *J. Thorac. Oncol.* **14**(6), 1032–1045 (2019).
42. Rajeshkumar, N. V. et al. MK-1775, a potent Wee1 inhibitor, synergizes with gemcitabine to achieve tumor regressions, selectively in p53-deficient pancreatic cancer xenografts. *Clin. Cancer Res.* **17**(9), 2799–2806 (2011).
43. Su, Y. L. et al. Inhibiting WEE1 augments the antitumor efficacy of cisplatin in urothelial carcinoma by enhancing the DNA damage process. *Cells* **12**(11), 1471 (2023).
44. Leijen, S. et al. Phase I study evaluating WEE1 inhibitor AZD1775 as monotherapy and in combination with gemcitabine, cisplatin, or carboplatin in patients with advanced solid tumors. *J. Clin. Oncol.* **34**(36), 4371–4380 (2016).
45. Lobo, J. et al. 53 and MDM2 expression in primary and metastatic testicular germ cell tumors: Association with clinical outcome. *Andrology* **8**(5), 1233–1242 (2020).
46. Keenan, T. E. et al. Clinical efficacy and molecular response correlates of the WEE1 inhibitor adavosertib combined with cisplatin in patients with metastatic triple-negative breast cancer. *Clin. Cancer Res.* **27**(4), 983–991 (2021).
47. Lheureux, S. et al. A randomized double-blind placebo-controlled phase II trial comparing gemcitabine monotherapy to gemcitabine in combination with Adavosertib in women with recurrent, platinum resistant epithelial ovarian cancer: A trial of the Princess Margaret, California, Chicago and Mayo Phase II Consortia (American Society of Clinical Oncology, 2019).
48. Lheureux, S. et al. Adavosertib plus gemcitabine for platinum-resistant or platinum-refractory recurrent ovarian cancer: A double-blind, randomised, placebo-controlled, phase 2 trial. *Lancet* **397**(10271), 281–292 (2021).
49. Port, M. et al. Micro-RNA expression in cisplatin resistant germ cell tumor cell lines. *Mol. Cancer*. **10**, 52 (2011).

50. Oechsle, K. et al. Preclinical and clinical activity of Sunitinib in patients with cisplatin-refractory or multiply relapsed germ cell tumors: a Canadian urologic oncology group/German testicular cancer study group cooperative study. *Ann. Oncol.* **22**(12), 2654–2660 (2011).
51. Fenske, A. E. et al. Cisplatin resistance induced in germ cell tumour cells is due to reduced susceptibility towards cell death but not to altered DNA damage induction or repair. *Cancer Lett.* **324**(2), 171–178 (2012).

Acknowledgements
The authors performed experiments at the Flow cytometry platform of the Department of Translational and Molecular Medicine of the University of Brescia.

Author contributions
M. Tamburello: Conceptualization, formal analysis, investigation, methodology, project administration, writing–original draft and editing. C. Boldini: Investigation, methodology and writing–original draft. (A) Abate and V. Salvi: formal analysis, writing–original draft and editing. F. Valcamonico, M. Laganà, D. Cosentini, N. R. Suardi, G. Mirabella and (B) Altieri: writing–original draft and editing. S. Sigala: Resources, funding acquisition, writing–review and editing. All authors reviewed the manuscript and approved the final version for submission.

Funding
This study was supported by the generous donations of the MO4MO and MoVa Associations, within the Movember 2022 and 2023 initiatives, and the Associations "Gli Amici di Robi" and "Associazione APS Michelangelo Barcella", in memory of their friends Roberto and Michelangelo.

Declarations

Competing interests
The authors declare no competing interests.

Additional information
Supplementary Information The online version contains supplementary material available at https://doi.org/10.1038/s41598-025-34904-5.

Correspondence and requests for materials should be addressed to A.A.